

Master in Photonics

MASTER THESIS WORK

**HIGH-COHERENCE LIGHT SOURCE AT
780nm, FOR ^{87}Rb TRAPPING AND
COOLING EXPERIMENTS**

Silvana Palacios Álvarez

Supervised by Dr. Morgan Mitchell (ICFO)

Presented on date 6th September, 2012

Registered at

ETSEP Escola Tècnica Superior
d'Enginyeria de Telecomunicació de Barcelona

High-coherence light source at 780nm, for ^{87}Rb trapping and cooling experiments.

Silvana Palacios Álvarez

The Institute of Photonic Sciences (ICFO), Barcelona

E-mail: silvana.palacios@icfo.es

Abstract. A master clock (frequency reference) for experiments related to cold and trapped rubidium atoms was developed. From a telecommunication fibre laser source at 1560nm, frequency-doubling was optimized to obtain an ultranarrow linewidth ($< 1\text{kHz}$) laser at 780nm with power larger than 100mW. Frequency-stabilization will implement an error signal resulting from modulation transfer spectroscopy.

Keywords: Fibre lasers, nonlinear optics, precision spectroscopy, atomic physics.

1. Introduction: The need of a frequency reference

Ultracold atoms have proven to be very useful in a long list of topics of physics including quantum simulators [1], optical clocks [2, 3] and metrology [4, 5]. Atomic sensors are currently the most sensitive detectors of low-frequency magnetic fields, and the combination of them with quantum non-demolition measurements, entanglement, squeezing, or non linear interactions [6, 7, 8] could provide us with instruments capable of measuring magnetic fields and its anomalies in space or earth [9], as well as detecting and mapping feeble brain magnetic fields that are imperceptible with currently employed SQUIDS [10, 11].

The aim of this project is to work with cold and trapped rubidium atoms for studying such light-matter interactions, this leads us to the development of a state-of-the-art atom trap, the first requirement of which is a highly-stable optical frequency reference; a master clock for the entire experiment.

In this thesis I report on the development of a very narrow linewidth laser source at 780nm (^{87}Rb D_2 transition line) by doubling a 1560nm fibre laser (section 3.1). The active stabilization of the source employs the D_2 line as a spectroscopic reference (section 3.2).

All the lasers for cooling and trapping will be frequency-stabilized by using the beat signal between them and our clock. The involved heterodyne locking will then give us several good lasers; when two lasers are locked together their relative linewidth becomes very narrow.

Since the master clock is the best reference of the lab, the estimation of its linewidth is done by implementing a self heterodyne detection. (section 2.1)

2. Light source

Fibre lasers can be constructed to be intrinsically single-longitudinal-mode with linewidths even below 1kHz, whereas extended cavity diode lasers (ECDL), being ubiquitous technology in atom physics, have linewidths of tens or hundreds of kHz. It is possible to achieve long-term stable operation of fibre lasers and to tune their emission frequency by changing temperature or applying tensile strain to the fibre. Erbium doped fibre laser systems operate in the 1530-1585nm wavelength range and offer the lowest phase and frequency noise and narrowest linewidth of the entire laser portfolio [12]. These properties make fibre lasers an attractive solution to our search for a reference laser, since a simple frequency doubling can provide us with our desired frequency.

Our master clock begins with a Koheras Adjustik and Boostik (Erbium Doped Fiber Amplifier, EDFA) systems by NKT Photonics. Their maximum powers are 40mW and 3W respectively. The emitted wavelength is 1560nm and the thermal tuning range of around 0.5nm. The piezo that stretches the fibre can change the wavelength by up to 22pm.

2.1. Linewidth Measurement

Characterization of laser properties, like the measurement of its linewidth, becomes more difficult the narrower the spectrum is. Typical optical spectrum analysers and scanning filter methods do not offer the resolution required, as a result, different techniques including frequency discriminator, self-heterodyne and recirculating delayed self-heterodyne detection have been developed [13, 14]. The knowledge of this feature and the possibility to monitor it allow to determine the behaviour of the Adjustik system with time, which is indispensable as it is our master clock.

We implemented the self-heterodyne technique which relies on mixing a laser with a delayed and frequency-shifted copy of itself, in contrast to true heterodyne detection, which mixes two different laser sources. Detecting the two spatially coherent beams on a photodiode gives rise to a beat note centred at the shift frequency (oscillating contribution to the mixing product), from this signal the linewidth of the laser can be retrieved.

Mathematically the total field to retrieve is then given by

$$E_T(t) = E(t) + \alpha E(t + \tau_d) \exp\{i\omega_0 t\}, \quad (1)$$

where τ_d is the delay time, ω_0 the shift frequency and α the ratio between field amplitudes. Assuming stationary fields the autocorrelation of the photocurrent depends only on the intensity correlation function of the total field (1), which is found to be [15]

$$G^{(2)}(\tau) = E_0^4 \left[(1 + \alpha^2)^2 + 2\alpha^2 \cos(\omega_0\tau)A \right], \text{ where}$$

$$A = \exp \left\{ -\frac{4}{\pi} \int_{-\infty}^{\infty} \sin^2 \left(\frac{\omega\tau}{2} \right) \sin^2 \left(\frac{\omega\tau_d}{2} \right) \frac{S_{\phi}(\omega)}{\omega^2} d\omega \right\}, \quad (2)$$

and $S_{\phi}(\omega)$ is the frequency noise spectrum of the source. It determine the linewidth of our source.

As stated by the Wiener-Khintchine theorem, one can deduce the power spectral density $\mathcal{S}(\omega)$ of the total field by Fourier transforming (2). $\mathcal{S}(\omega)$ can be observable with a Spectrum Analyser, and from it, it is possible to infer the dependence of the frequency noise with frequency.

In order to simplify the interpretation of the detected signal in terms of the laser linewidth, the delay has to be large enough so that both beams are essentially uncorrelated. In this case the output spectrum becomes a self-convolution of the laser output spectrum [13].

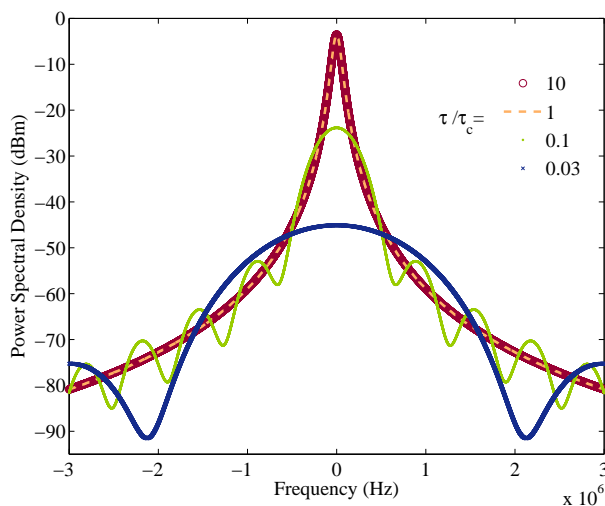


Figure 1. Calculated spectrum of the self-heterodyne signal for different delay times. $\tau_d/\tau_c \ll 1$ corresponds to a function with large oscillations whereas $\tau_d/\tau_c \geq 1$ is good approximation to a Lorentzian function. $\tau_c = 1ms$. (Colour on-line)

For lasers exhibiting only white frequency noise, this constraint translates in a delay larger than the coherence time. As shown in figure 1, $\mathcal{S}(\omega)$ describes a distorted autocorrelation; such a distortion becomes small when the delay is larger than the coherence time.

In our case the wavelength of the source lives in a telecommunication window for which attenuation in typical single-mode fibres is only 0.19dB/km. Therefore, introducing a delay of 0.5ms (100km of fibre) only attenuate by 19dB the light passing through. Note that this would not be attractive for direct measurements of 780nm because losses

increase to 4dB/km. To overcome such a limitation more elaborate techniques such as loss-compensated recirculating self-heterodyne detection have been implemented [16, 17].

White noise is the contribution from quantum phase fluctuations [18, 19] and can be written as $S_{\dot{\phi}}(\omega) = S_0$ constant. Substituting S_0 and Fourier transforming (2) the power spectral density becomes

$$\mathcal{S}(\omega) \propto E_0^4 \left(2\alpha^2 \exp\{-S_0\tau_d\} \delta(\omega - \omega_0) + \frac{4\alpha^2 S_0}{S_0^2 + (\omega - \omega_0)^2} \right. \\ \left. \times \left[1 - \exp\{-S_0\tau_d\} \left\{ \cos((\omega - \omega_0)\tau_d) + \frac{S_0}{\omega - \omega_0} \sin((\omega - \omega_0)\tau_d) \right\} \right] \right), \quad (3)$$

with $S_0 = 2\pi\Delta\nu_{\text{LF}}/2$. According to equation (3) delays much larger than $1/S_0$ produce a Lorentzian lineshape of the signal, the full width at half maximum (FWHM) of which ($\Delta\nu_{\text{LF}}$) is twice the FWHM of the laser itself ($\Delta\nu_{\text{L}}$) [13]. Figure 1 exhibits the dependence of the beat signal and the introduced delay, showing that a delay larger than the coherence time $\tau_c = 2/\Delta\nu_{\text{LF}}$ is necessary to read a Lorentzian dependence with frequency.

In the case of fibre lasers, it has been shown that its frequency noise has also a low-frequency contribution to the spectrum, which is substantially due to pump-noise related to temperature fluctuations. This implies that a delay slightly larger than the coherence time may underestimate the measured linewidth. If such a low frequency contribution can be approximated as a constant up to a cut-off frequency, the resulting power spectral density corresponds to a Gaussian lineshape [20].

According to the manufacturer we can expect both a Lorentzian profile and a Gaussian contribution in $\mathcal{S}(\omega)$. Such a behaviour can be obtained by writing the frequency noise spectrum as:

$$S_{\dot{\phi}}(\omega) = S_0 + \frac{k}{|\omega|}, \quad (4)$$

as successfully has been modelled in some previous works [17]. Assuming (4), $\mathcal{S}(\omega)$ can be described as a Voigt function $V(z)$ being the convolution of a Lorentzian with FWHM $\Delta\nu_{\text{LF}}$ and a Gaussian with FWHM $\Delta\nu_{\text{GF}}$ ‡ [15]. Such a function can be represented as: [21]

$$V(z) = \Re\{\exp(z^2) \operatorname{erfc}(z)\}, \quad \text{where} \quad (5) \\ z = \sqrt{\ln(2)} \left[\frac{\Delta\nu_{\text{LF}}}{\Delta\nu_{\text{GF}}} + \mathbf{i} \frac{2(\nu - \nu_0)}{\Delta\nu_{\text{GF}}} \right].$$

By fitting (5) to the measured spectrum of the beat signal we can estimate $\Delta\nu_{\text{LF}}$ and $\Delta\nu_{\text{GF}}$, and in turn, $\Delta\nu_{\text{L}} = \Delta\nu_{\text{LF}}/2$ and $\Delta\nu_{\text{G}} = \sqrt{2}\Delta\nu_{\text{GF}}/2$ approximately [15].

‡ Mercer found an empirical Gaussian approximation of $\mathcal{S}(\omega)$ for cases where $k\tau_d^2/\pi \gg 1$

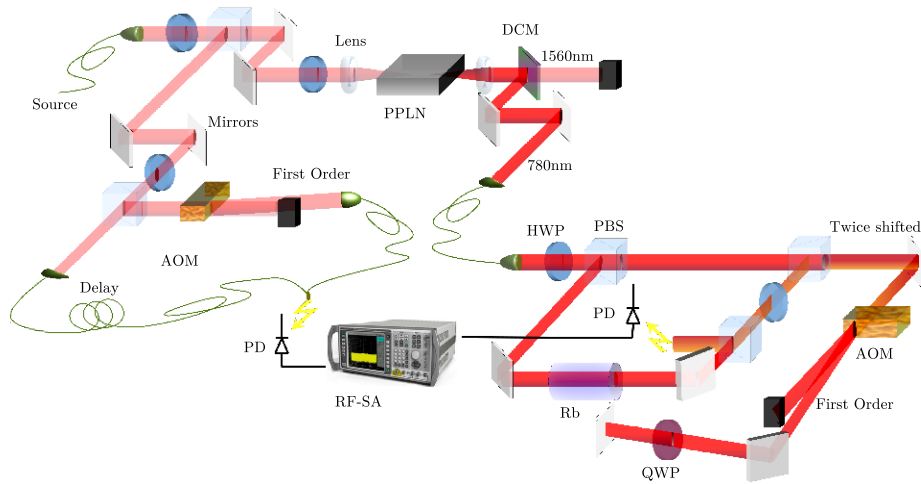


Figure 2. Schematic setup for linewidth measurement, frequency doubling and frequency stabilization. Middle left shows linewidth measurement through delayed self-heterodyne detection. Top depicts frequency doubling by means of a PPLN crystal. Bottom right shows modulation transfer spectroscopy to generate an error signal for frequency stabilization of the fibre laser. AOM: acousto-optic modulator, PBS: polarizing beam-splitter, QWP: quarter-wave plate, HWP: half-wave plate, DCM: dichroic mirror PD: photodiode, RF-SA: RF spectrum analyser.

Middle left part of figure 2 shows the arrangement for self-heterodyne detection: the source is split into two paths, one is frequency shifted by means of an AOM with central frequency 110MHz (Crystal Technology), the second path is 0.5ms delayed by traversing 100km of fibre (Corning SMF-28). Afterwards both beams are recombined and detected with a photodiode (Thorlabs PDA10CF). The signal from the PDA is decompose in its RF and DC components (Minicircuits Bias Tee), the RF signal is sent to an RF Spectrum Analyser and the DC to an oscilloscope, the last signal is used to maximize the detection and to find the ratio between the intensity of the two beams (α^2).

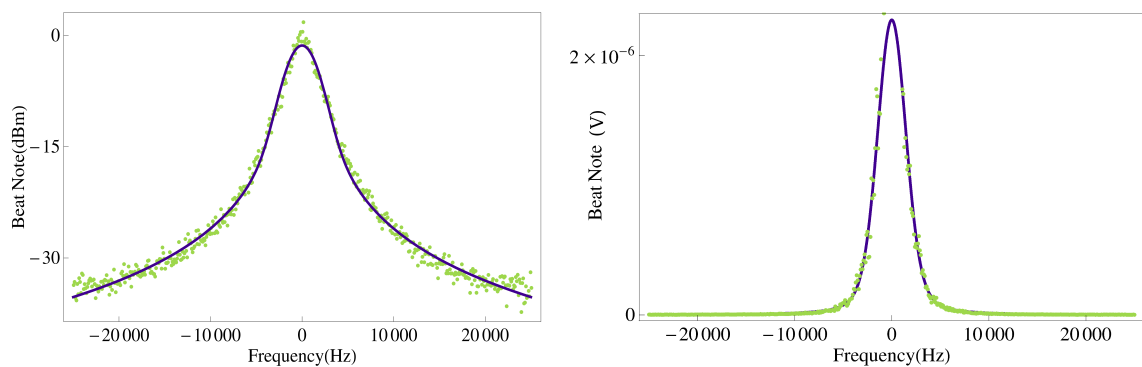


Figure 3. Green dots: measured beat note of a field as given in (1) with $\tau_d = 0.5\text{ms}$, $\omega_0 = 2\pi 110\text{MHz}$, $\alpha^2 = 3/160$ and the total power being 40mW. Violet line: automatic Voigt fit according to (5).

Green dots in figure 3 (frequency is centred at $\omega_0 = 2\pi \times 110\text{MHz}$) show the measured signal in the SA, while its resolution bandwidth is 10Hz and video bandwidth is 3Hz. The AOM was driven by a clock frequency generator at 110MHz, the observed bandwidth of which was only limited by the maximum resolution of the SA. The AOM can also be driven by a standard VCO provided that its bandwidth is much narrower than the expected bandwidth of the beat note, in this way the measurement of the spectrum won't be limited by it.

Following (5), an automatic fit (violet lines in figure 3) gives the values: $\Delta\nu_{\text{LF}} = 953\text{Hz}$ and $\Delta\nu_{\text{GF}} = 2986\text{Hz}$, therefore, the Lorentzian and Gaussian FWHM of our laser are

$$\begin{aligned}\Delta\nu_{\text{L}} &= 476\text{Hz}, \\ \Delta\nu_{\text{G}} &= 2112\text{Hz},\end{aligned}$$

respectively. We have to remark that the measured $\Delta\nu_{\text{L}}$ exceeds the maximum value given by the manufacturer by a factor of two. Notice that points on the top of the figure 3 do not fall on the line. They are the contribution of the delta function term in (3), the high of which is determined by the prefactor $\exp\{-S_0\tau_d\} \simeq 0.04$.

3. Beam at ^{87}Rb D₂ transition line

3.1. Frequency doubling

Generation of light in a suitable colour to interact with the ^{87}Rb D₂ line takes place in a nonlinear material where light at 1560nm is doubled into light at 780nm (SHG).

Periodically polarised bulk crystals and waveguides, where the phase-velocity mismatch of the interaction is compensated, represent a powerful tool to convert light into different colours, polarization, etc. The former ones can accept higher powers and have much larger apertures, nevertheless, diffraction inside them limits the maximum efficiency one can achieve, since very tightly focus beams do not travel long distances with the same momentum distribution. In the case of waveguides, since light is strongly confined, it is possible to fabricate arbitrary long guides in order to increase the total efficiency of the process, in addition, the conversion efficiency scales quadratically with the traversed distance instead of linearly as in a bulk crystal.

Our main interest is to get as much power as possible inheriting the properties of the pump laser, in this sense the limitation on input powers for waveguides make the bulk crystal to be the better option. Among the different commercial solutions, the type I configuration in Lithium Niobate (LiNbO_3) exhibits the largest nonlinear coefficient for this aim ($d_{33} = 25\text{pm/V}$ at 1064nm). The efficiency of our particular crystal (HCP Photonics PPLN crystal, grating period $19.48\mu\text{m}$ to work near 82°C , 50mm long and doped with MgO to minimize damage in the crystal due to high pump powers) is, according to the fabricator around $\eta = P^{\text{SHG}}/P^2 = 2\%/W$ and according to our measurements (figure 4) $1.9\%/W$.

Top part of figure 2 shows the setup to convert the telecommunication wavelength into light at 780nm. The beam is focussed into the crystal and re-collimated by means of a pair of lenses. The remaining 1560nm beam is separated with a dichroic mirror and the 780nm light is fibre coupled.

Following the Boyd-Kleinman optimization of the process we are interested in, the total length of the crystal has to be 2.84 times $2z_R$, where z_R is the Rayleigh length associated to the beam diameter and the focal length of the focusing lens [22]. For 50mm crystal length the lenses that satisfy such an optimization have a focal length of around 60mm, knowing that our beam diameter is 2.1mm.

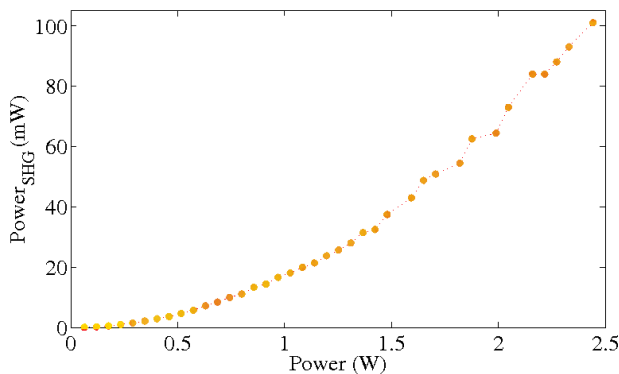


Figure 4. Power of the converted signal at 780nm (SHG) as function of pump power (1560nm) while maintaining constant temperature (87.5°C). The behaviour shows a quadratic dependence, as expected.

Assuming the frequency conversion is instantaneous, $E(t)^{\text{SHG}} \propto E(t)^2$, therefore, the phase of the second harmonic is twice the phase of the fundamental beam. This means: $\Delta\nu_L^{\text{SHG}} = 2\Delta\nu_L = 953\text{Hz}$.

The Boostik system emitting only 2.5W of its power and after being properly focused into a nonlinear PPLN crystal gives rise to a light source of linearly polarized light at 780nm with ultranarrow linewidth $< 1\text{kHz}$ and power of 105mW, which is equivalent to a 3B class laser (see figure 4).

3.2. Laser Locking

The free-running linewidth, or short-term stability of a laser, is often not adequate for many applications regarding atom physics. Electronic noise, temperature fluctuations and many other factors can induce changes over time of the frequency emitted by a laser. Since manipulation of atomic systems require a good frequency stability, extra feedback control systems have to be implemented. Active laser stabilization has been successfully applied using many different error signals coming in general from a spectroscopy technique. The pump-probe schemes such as saturated absorption or mod-

ulation transfer spectroscopy achieve sub-Doppler resolution, the last one additionally generates dispersive-like lineshapes sit on a flat background, so one can well distinguish between close hyperfine levels [23, 25]. In order to take advantage of such characteristics we implemented the modulation transfer spectroscopy in the locking system.

Modulation Transfer spectroscopy

The typical configuration of this technique is: as shown in the right bottom part of figure 2 the optical arrangement consists of two beams that overlap inside a rubidium cell. Both are counter-propagating and the ratio of their intensities is larger than 1. The weaker beam (probe) comes directly from the second harmonic beam, the more intense (pump) is first frequency-shifted by means of a double-pass frequency-modulated AOM which creates sidebands around the carrier frequency. After traversing the cell, the probe beam is detected on a PD.

The AOM (Crystal Technology 3080-122) is driven with a VCO at $f_c = 80\text{MHz}$ (Minicircuits ZX95-78+) modulated with a sinusoidal wave at $f_m = 3\text{MHz}$ from a frequency generator. The pump beam traversing such an AOM is frequency modulated acquiring an extra phase of $2\pi f_c t + \delta \sin(2\pi f_m t)$, where δ is the modulation index. For a double pass the resulting pump beam is

$$E_{\text{DP}}(t) \propto E_0 \sin \{2\pi(\nu + 2f_c)t + 2\delta \sin(2\pi f_m t)\},$$

that for a small modulation index can be approximated as:

$$E_{\text{DP}}(t) \simeq E_0 \{ \delta \sin[2\pi(\nu + 2f_c + f_m)t] + \sin[2\pi(\nu + 2f_c)t] - \delta \sin[2\pi(\nu + 2f_c - f_m)t] \} \quad (6)$$

Once the two beams overlap a four-wave mixing (FWM) process between two pump bands and the probe generate a sideband on the probe. This is, the modulation is transferred from the pump to the probe. The strongest modulation transfer signals are observed for closed transitions where FWM is very efficient as atoms can not relax to other ground states [26].

The modulation transfer signal only takes place when the sub-Doppler resonance condition is satisfied, this gives a lineshape baseline stability that is almost independent of the residual linear-absorption effect; a zero background signal.

Detection on the PD is the beat signal between the middle frequency of the probe beam with each of the sidebands, and can be written as [25]:

$$\mathcal{S}^{\text{MT}}(\omega_m) \propto [L_{-1} - L_{-1/2} + L_{1/2} - L_1] \cos(\omega_m t + \phi) + [D_{-1} - D_{-1/2} - D_{1/2} + D_1] \sin(\omega_m t + \phi), \quad (7)$$

where for a linewidth natural linewidth Γ , a frequency detuning from the line centre Δ , and a detector phase with respect to the modulation field applied to the pump laser ϕ :

$$L_k = \frac{\Gamma^2}{\Gamma^2 + (\Delta - k\omega_m)^2}, \text{ and}$$

$$D_k = \frac{\Gamma(\Delta - k\omega_m)}{\Gamma^2 + (\Delta - k\omega_m)^2}.$$

In (7) the sine term represents the quadrature component and the cosine term the in-phase component of the signal. This means that by choosing ϕ to select only the quadrature (in-phase) term it is possible to recover the absorption (dispersion) component of the sub-Doppler resonance.

For $\omega_m \leq \Gamma$ both, the absorption and dispersion signals, have a similar lineshape with a large gradient when crossing the centre of the resonance [25]. In particular, $f_m = 3\text{MHz}$ was found to be optimal for locking the cooling transition in $^{87}\text{Rb D}_2$ ($F = 2 \rightarrow F' = 3$) [24].

Demodulating (Minicircuits ZAD-6+) the signal on the PD (Thorlabs PDA10A-EC) using a phase-shifted copy of the signal frequency-modulating the VCO, and properly filtering, one can obtain a suitable error signal to feed the closed-loop controller of the laser frequency.

4. Final Remarks

A sub-kHz linewidth laser emitting at 780nm and having a power larger than 100mW was developed. Frequency stabilization of such a system takes an error signal resulting from modulation transfer spectroscopy on $^{87}\text{Rb D}_2$ line; electronics related to the closed-loop controller are currently being implemented.

After the source is actively stabilized we will proceed to the stabilization of the rest of the lasers (ECDL) for cooling and trapping rubidium atoms.

Acknowledgements

This work was funded by the European Research Council and Fundació CELLEX under the AQUMET project.

References

- [1] Cirac, I. and Zoller, P. *How to Manipulate Cold Atoms*. 2003 Science **301**, 5630 176
- [2] Wilpers, G. et al. *Optical Clock with Ultracold Neutral Atoms*. 2002 Phys. Rev. Lett. **89**, 230801
- [3] Blatt, S. et al. *New Limits on Coupling of Fundamental Constants to Gravity Using ^{87}Sr Optical Lattice Clocks*. 2008 Phys. Rev. Lett. **100**, 140801
- [4] Bordé, C. *Base units of the SI, fundamental constants and modern quantum physics*. 2005 Phil. Trans. R. Soc. A **363**, 1834 2177
- [5] Udem, T. et al. *Optical frequency metrology*. 2002 Nature **416**, 233

- [6] Koschorreck, M. et al. *Sub-projection-noise sensitivity in broadband atomic magnetometry*. 2010 Phys. Rev. Lett. **104**, 093602
- [7] Sewell, R. et al. *Spin-squeezing of a large-spin system via QND measurement*. 2011 arXiv:1111.6969v2
- [8] Napolitano, M. et al. *Interaction-based quantum metrology showing scaling beyond the Heisenberg limit*. 2010 Nature **471**, 486
- [9] Budker, D. and Romalis, M. *Optical Magnetometry*. 2007 Nature Physics **3**, 227
- [10] Xia, H. et al. *Magnetoencephalography with an atomic magnetometer*. 2006 App. Phys. Lett. **89**, 211104
- [11] Hämäläinen, M. *Magnetoencephalography theory, instrumentation, and applications to noninvasive studies of the working human brain*. 1993 Rev. Mod. Phys. **65**, 413 (1993)
- [12] *AdjustiK Benchtop - Narrow Linewidth, Low Noise, Single Frequency Fiber Laser* from <http://www.nktphotonics.com/>
- [13] Okoshi, T. et al. *Novel method for high resolution measurement of laser output spectrum*. 1980 Electron. Lett. **16**, 16 630
- [14] Tsuchida, H. *Simple technique for improving the resolution of the delayed self-heterodyne method*. 1990 Opt. Lett. **15**, 11 640
- [15] Mercer L. *1/f Frequency Noise Effects on Self-Heterodyne Linewidth Measurements*. 1991 J. Lightwave Technol. **9**, 4
- [16] Park, N. et al. *Linewidth and frequency jitter measurement of an erbium-doped fiber ring laser by using loss-compensated, delayed self-heterodyne interferometer*. 1992 Opt. Lett. **17**, 18 1274
- [17] Chen X. *Ultra-Narrow Laser Linewidth Measurement*. 2006 Thesis. Faculty of the Virginia Polytechnic Institute and State University. Virginia.
- [18] Gallion, P. B. and DeBarge, G. *Quantum phase noise and field correlation in single frequency semiconductor laser systems*. 1984. IEEE J. of Quantum Electron. **QE-20**, 343
- [19] Richter, L. et al. *Linewidth Determination from Self-Heterodyne Measurements with Subcoherence Delay Times*. 1986. IEEE J. of Quantum Electron., **QE-22**, 11 2070
- [20] Horak P. and Loh W. H. *On the delayed self-heterodyne interferometric technique for determining the linewidth of fiber lasers*. 2006 Opt. Exp. **14**, 9 3923
- [21] *Voigt functions* Digital Library of Mathematical Functions. 2012-03-23. National Institute of Standards and Technology from <http://dlmf.nist.gov/7.19>
- [22] Boyd, G. and Kleinman, D. *Parametric Interaction of Focused Gaussian Light Beams*. 1968 J. Appl. Phys. **39**, 8 3597
- [23] Negnevitsky, V. *FPGA-based laser stabilisation using modulation transfer spectroscopy*. 2010 Thesis. Monash University. Australia.
- [24] Negnevitsky, V. and Turner L. *Wideband laser locking to an atomic reference with modulation transfer spectroscopy*. 2012 arXiv:1204.5240v1
- [25] McCarron, D. *Modulation transfer spectroscopy in atomic rubidium*. 2008 arXiv:0805.2708v3
- [26] Ducloy M. and Bloch D. *Theory of degenerate four-wave mixing in resonant Doppler-broadened media. II. Doppler-free heterodyne spectroscopy via collinear four-wave mixing in two- and three-level systems*. 1982 J. Physique **43**, 57